Impact of Amyotrophic Lateral Sclerosis on Slow Tonic Myofiber Composition in Human Extraocular Muscles

Anton E. Tjust,[1,2] Adam Danielsson,[1] Peter M. Andersen,[3] Thomas Brännström,[4] and Fatima Pedrosa Domellöf[1,2]

[1]Department of Integrative Medical Biology, Umeå University, Umeå, Sweden
[2]Department of Clinical Science, Ophthalmology, Umeå University, Umeå, Sweden
[3]Department of Pharmacology and Clinical Neuroscience, Umeå University, Umeå, Sweden
[4]Department of Medical Biosciences, Umeå University, Umeå, Sweden

Correspondence: Fatima Pedrosa Domellöf, Department of Clinical Science, Ophthalmology, Umeå University, Umeå 90185, Sweden; fatima.pedrosa-domellof@umu.se.

Submitted: April 23, 2017
Accepted: June 19, 2017

Citation: Tjust AE, Danielsson A, Andersen PM, Brännström T, Pedrosa Domellöf F. Impact of amyotrophic lateral sclerosis on slow tonic myofiber composition in human extraocular muscles. *Invest Ophthalmol Vis Sci*. 2017;58:3708–3715. DOI:10.1167/iovs.17-22098

Purpose. To analyze the proportion and cross-sectional area of myofibers containing myosin heavy chain slow-twitch (MyHCI) and myosin heavy chain slow tonic (MyHCsto) in extraocular muscles of autopsied amyotrophic lateral sclerosis (ALS) patients with either spinal or bulbar site of disease onset.

Methods. Whole-muscle cross sections from the middle portion of the medial rectus were labeled with antibodies against MyHCI or MyHCsto and laminin. Myofibers labeled with the MyHC antibodies (MyHCI+sto) and the total number of myofibers were quantified in the orbital and global layer of 6 control individuals and 18 ALS patients. The cross-sectional area of myofibers labeled for either MyHC was quantified in 130 to 472 fibers/individual in the orbital and in 180 to 573 fibers/individual in the global layer of each specimen.

Results. The proportion of MyHCI+sto myofibers was significantly smaller in the orbital and global layer of ALS compared to control individuals. MyHCI+sto myofibers were significantly smaller in the global layer than in the orbital layer of ALS, whereas they were of similar size in control subjects. The decreased proportion of MyHCI+sto fibers correlated significantly with the age of death, but not disease duration, in patients who had the bulbar-onset variant of ALS but not in patients with spinal variant.

Conclusions. ALS, regardless of site of onset, involves a loss of myofibers containing MyHCI+sto. Only in bulbar-onset cases did aging seem to play a role in the pathophysiological processes underlying the loss of MyHCI+sto fibers.

Keywords: amyotrophic lateral sclerosis, extraocular muscles, MyH14, slow tonic, muscle fibers

Amyotrophic lateral sclerosis (ALS) is a progressive, neurodegenerative heterogeneous syndrome characterized by adult-onset loss of primarily motor neurons in the somatic nervous system. It leads to degeneration of upper and lower motor neurons, resulting in muscle atrophy, paresis, and loss of tendon reflexes.[1] ALS usually starts in the upper or lower limbs with the symptoms outlined above, and this is termed "spinal-onset" or "classic" ALS.[1,2] The disease runs a progressive course, with more and more adjacent spinal levels becoming involved. In approximately 25% of cases, the first symptoms of the disease will manifest in the head and neck region, primarily affecting muscles of articulation and mastication innervated by the motor neurons in the nuclei of the cranial nerves; this is referred to as bulbar-onset ALS.[1] There is no effective treatment at present and eventually the respiratory muscles become affected and the patient dies from hypercapnia and/or pneumonia. The median survival after symptom onset is 3 to 5 years, but 5% to 10% of patients survive for 10 years or more, even without treatment, usually severely incapacitated.[1]

One remarkable feature of ALS already recognized by Charcot and Joffroy[2] is the noticeable preservation of eye motility in many ALS patients.[3] As a consequence, some patients who are otherwise paralytic can communicate with eye-controlled devices. Occasionally, disturbances in eye motility do occur, especially in patients who have survived longer with the help of invasive ventilation.[4,5] But even in such cases, the disturbances usually appear to be of supranuclear origin, and complete paralysis, external ophthalmoplegia, is absent in all but a small number of reported cases.[4] This is further supported by neuropathologic studies reporting that motor neuron loss in the oculomotor nuclei is infrequent.[6,7] We have previously demonstrated that the extraocular muscles (EOMs) of autopsied ALS patients are remarkably well preserved in comparison to their limb muscles.[8] One of the findings from that study was an apparent decrease in myofibers labeled for the myosin heavy chain (MyHC) slow tonic isoform but a preserved labeling of myofibers containing the MyHC heavy chain slow-twitch (MyHCI) isoform. Because of the low number of patients available and the extensive variability in MyHC changes between individual muscles and patients, a thorough quantification of MyHC slow tonic (MyHCsto) myofibers and correlation with the clinical phenotypes of the patients were not possible at that time.[8]

Table. Clinical Characteristics of the Studied ALS Patients

Patient	Sex	Age at Onset	Site of Onset	Disease Duration, mo	Age at Death	Disease Mutation(s)
1	M	48	Leg	316	74	*SOD1*^{D90A} homozygous
2	F	52	Leg	131	63	*SOD1*^{D90A} homozygous
3	F	53	Hand	11	54	*C9orf72* expansion
4	M	58	Leg	8	59	*C9orf72* expansion
5	F	60	Hand	13	61	Not known
6	M	62	Hand	58	66	Not known
7	M	67	Leg	34	69	*C9orf72* expansion
8	M	69	Hand	15	70	Not known
9	F	72	Hand	10	73	*SOD1*^{A4V} heterozygous
10	M	77	Hand	29	79	Not known
11	F	55	Bulbar	34	58	Not known
12	M	55	Bulbar	42	59	*VAPB*^{S160delS}
13	M	60	Bulbar	64	65	Not known
14	F	63	Bulbar	13	64	Not known
15	F	64	Bulbar	58	69	Not known
16	F	71	Bulbar	34	74	*C9orf72* expansion
17	M	75	Bulbar	16	77	Not known
18	F	79	Bulbar	10	80	Not known

Age of onset, disease duration, and age at death are reported in full lived years/months. Patients 1 and 2 were siblings. Both received intermittent noninvasive ventilation for some years. All patients were DNA screened for a panel of known ALS genes (details available upon request). C9orf72 expansion implies a heterozygous large GGGGCC-hexanucleotide expansion in intron 1 of *C9orf72*.

Even though there are some changes in morphology and MyHC composition in the EOMs,[8] innervation of the neuromuscular junctions is preserved both in ALS patients[9] and in the most commonly used transgenic mouse model of ALS, the tghSOD1^{G93A} mouse.[10] Actual loss of the motor neuron cell body appears to be a late phenomenon in ALS. In animal studies, the motor neuron loss is preceded by a period of progressive loss of contacts between axons and myofibers at the neuromuscular junction and retraction of peripheral axons, preceding symptom onset.[11,12] Therefore, studying changes at the muscle–tissue level may reveal more subtle signs of disease involvement, as well as compensatory mechanisms that may be of relevance for disease progression. Understanding the basis for the resilient traits of the EOMs and their motor neurons may provide new clues to mechanisms that could be of importance to slow down the progression of ALS in other parts of the motor system.

In the EOMs, slow myofibers are multiply innervated and also have tonic properties, reflected in their MyHCsto content.[13,14] These multiply innervated fibers (MIFs) are present in both the orbital and global layers of the EOMs and have several neuromuscular junctions along the length of each individual muscle fiber and, in the orbital layer, more than one motor neuron innervating the same myofiber.[15] This capacity to maintain several neuromuscular junctions on a single myofiber and share synapses between different motor neurons could perhaps make these muscle fibers less vulnerable in ALS. Furthermore, the motor neurons of EOM MIFs are located in a separate neuroanatomic niche and display a different repertoire of surface markers than other motor neurons do, suggesting that they may have distinct constitutive properties.[16–18]

We investigated the effect of ALS on MIFs in the orbital and global layer of ALS patients by analyzing the proportions and sizes of myofibers containing MyHCI and MyHCsto. We also investigated whether eventual changes in the MyHC composition correlated with known clinical parameters of the patients, to investigate whether the relative sparing of EOMs was manifested differently in spinal- versus bulbar-onset ALS.

Methods

Muscle Samples

Eighteen ($n = 18$) medial rectus muscles were collected post mortem from nine male and nine female terminal ALS patients (ages at death 54–80). All patients were diagnosed in accordance with the EFNS criteria for managing ALS.[19] The clinical characteristics of the ALS patients are summarized in the Table. Six ($n = 6$) medial rectus EOMs, collected post mortem from one female and five males (age 42–82), served as control. None of the control subjects were known to suffer from any neurologic or muscular disease. The EOMs were collected following approval of the study by the Medical Ethical Review Board. Informed consent was obtained from the patients themselves ante mortem or following the passing of the patient, from the next of kin, in accordance with relevant Swedish legislation and in accordance with the Declaration of Helsinki.

At autopsy, after removal of any orbital fat and visible connective tissue, whole EOMs were oriented and mounted longitudinally on a piece of foil-wrapped cardboard, using OCT cryomount (HistoLab Products AB, Gothenburg, Sweden). Muscle samples were quickly frozen in liquid propane chilled with liquid nitrogen. After freezing, samples were stored at –80°C until sectioning.

The longitudinally frozen muscles were placed in a Leica CM3050 cryostat (Leica Biosystems, Nussloch, Germany) set at –23°C. With a chilled razor blade, the midportion of the muscle was cut and then mounted for cross-sectioning. Whole EOM serial cross sections were cut from the middle portion, 5 μm thick, and collected on gelatin-covered glass slides. Slides were kept at –20°C until processed for immunofluorescence.

Immunofluorescence Staining. In brief, slides were brought to room temperature and left to dry for 20 minutes. Then, slides were rinsed for 3 × 5 minutes in phosphate-buffered saline (PBS), followed by 15 minutes of incubation with donkey normal serum at room temperature. Afterward, sections were incubated with a sheep polyclonal antibody against laminin (1:15,000, PC128; The Binding Site Group Ltd., Birmingham, UK) overnight at +4°C. On the next day, the

sections were brought to room temperature, rinsed, and incubated with normal serum (as above) and incubated with a donkey anti-sheep Alexa 647 secondary antibody (1:300, No. 713-605-147; Jackson Immunoresearch, West Grove, PA, USA) for 30 minutes at 37°C. Following this, the sections were rinsed and incubated as above with a mouse monoclonal antibody against MyHCI (1:50, A4.951; Developmental Studies Hybridoma Bank, Iowa City, IA, USA) and a rabbit polyclonal antibody against MYH14/7b[20] (here referred to as MyHCsto, 1:500, generously provided by Stefano Schiaffino, University of Padova, Padova, Italy) for 60 minutes at 37°C. Subsequently, sections were rinsed and incubated as above with a donkey anti-mouse FITC secondary antibody (1:100, No. 711-095-151; Jackson Immunoresearch) and a donkey anti-rabbit RRX secondary antibody (1:500, No. 711-295-152; Jackson Immunoresearch) for 30 minutes at 37°C. Lastly, sections were rinsed in PBS and mounted with coverslips using Vectashield Antifade mounting medium (Vector Laboratories, Inc., Burlingame, CA, USA). Secondary antibody controls were used to verify the labeling of the primary antibodies.

Microscopy. All slides were analyzed with a Leica DM 6000 B microscope (Leica Microsystems, Wetzlar, Germany) equipped with a motorized stage. A set of images (1392 × 1040 pixels) together covering the whole cross section of each specimen was captured using a ×20 objective and a digital montage was automatically assembled. The boundary between the orbital and global layers was drawn on the whole-section digital montage.

From the montage image, images were randomized and quantified until at least 1800 myofibers from the global and 1500 myofibers from the orbital layer, respectively, had been analyzed with regard to MyHC composition. On each image, a counting frame for unbiased quantification of variable-sized structures[21] was used.

The total number of myofibers present within the counting area was recorded, together with the number of myofibers labeled with antibodies against MyHCI, MyHCsto, or both MyHCs (MyHCI+sto). From this, the proportion of each type of fiber to the total was calculated.

The cross-sectional area (CSA) of individual myofibers labeled with either myosin antibody was measured, based on the laminin-labeled outline of the myofiber, using Qwin Standard V.3.5.1 software (Leica Microsystems Ltd., Heerbrugg, Switzterland) on a randomized subset of images from each layer. CSA was calculated from 180 to 573 myosin-labeled myofibers/individual from the global layer and 130 to 472 myosin-labeled myofibers/individual from the orbital layer of each subject by tracing the perimeter of each myofiber, detected with laminin labeling, converting the enclosed pixels to a surface area (expressed in μm^2).

Statistics

Statistical analyses and tests were carried out in the SPSS Statistics software (IBM, Armonk, NY, USA). Statistical comparisons between control and ALS groups were done as planned contrast tests with two levels of hypotheses: (1) Did ALS patients differ from control subjects, and (2) did ALS patients with bulbar or spinal onset differ from each other? All estimates were tested for nonnormal distributions using a Shapiro-Wilk test and Q-Q plots, with groups stratified down to the lowest expected level (controls, spinal-onset, and bulbar-onset). The test suggested that the proportion and CSA of MyHCI+sto fibers in control subjects, as well as the CSA of MyHCI+sto fibers in bulbar-onset patients, was nonnormal in the orbital layer. Based on graphic analysis, these estimates looked positively skewed with a possible heavy-tailed distribution. Since the underlying distribution for our estimates was unknown and likely to be nonnormal in some cases, we did all subsequent statistic tests of subject–group differences with a bias-corrected accelerated bootstrap sampling,[22] with the sampling size set at 8000 runs. Testing of the three groups, based on the planned contrasts outlined above, was done with 1-way ANOVA with the above-mentioned bootstrap. Testing of differences between fiber types and the orbital and global layer within subject groups (controls, spinal-onset, and bulbar-onset) was performed with a paired *t*-test or, when appropriate due to nonnormality, a Wilcoxon matched-pair signed-rank test. Sidak correction was used with a subsequent *P* value adjustment for multiple comparisons where applicable. Estimates are presented as arithmetic mean ± 1 standard deviation and, where applicable, lower and upper bootstrap 95%CI (confidence interval).

A regression analysis was performed to investigate whether disease duration, age of onset, or age of death correlated with MyHCI+sto proportion in the global layer. We did the regression analysis on all three groups (controls and spinal-onset and bulbar-onset patients) separately. The residuals of cases were normally distributed in all groups, and no case had a standardized residual $\leq \pm 1.96$. Also, Cook's distance was <1.0 for all cases. For estimation of *P* values and a 95%CI interval of the regression coefficient (β), a bias-corrected and accelerated CI was generated through an 8000-run bootstrap. To estimate generalizability of the model to the parent population, R^2 was adjusted with Darlington's formula.[23] *P* values for all tests were considered significant for $P < 0.05$.

Results

Myofibers labeled with both MyHC antibodies (MyHCI+sto myofibers) were present across the whole EOM cross section and evenly distributed in both ALS and age-matched control subjects. Labeled myofibers did not appear to cluster in either group, but some areas in the global layer of ALS patients had very few myofibers labeled with either antibody. Those few labeled myofibers present in these areas were notably smaller than labeled myofibers in other areas.

MyHCI and MyHCsto in Control EOMs

In the medial rectus muscle of control subjects, 12% to 18% of all myofibers were colabeled for MyHCsto and MyHCI and evenly distributed across the whole muscle cross section. In all control individuals, a clear difference in labeling intensity with the antibodies against MyHCsto and MyHCI was noted between the orbital and global layers. MyHCsto labeling was consistently strong in the orbital layer, but generally weak in the global layer. Conversely, MyHCI labeling was consistently strong in the global layer but more moderate in the orbital layer (Fig. 1).

Almost every myofiber (>99.5%) labeled for MyHCsto was also labeled for MyHCI in the middle portion of the medial rectus muscle (Fig. 1). These double-labeled MyHCI+sto myofibers corresponded to 14.0 ± 2.4% of the total number of myofibers in the global layer and 17.1 ± 3.0% in the orbital layer (Fig. 2). In addition, there were myofibers in the orbital and global layer labeled for MyHCI but not for MyHCsto. These myofibers made up 1.9 ± 0.6% of the total number of myofibers in the global layer and 0.8 ± 0.4% of the total number of myofibers in the orbital layer (Fig. 2).

The mean CSA of MyHCI+sto myofibers was similar ($P < 0.712$) in the global layer (186 ± 72 μm^2) and orbital layer (188 ± 39 μm^2) (Fig. 3). The mean CSA of MyHCI-only myofibers was also similar ($P < 0.712$) in the global layer (157 ± 17 μm^2) and orbital layer (144 ± 45 μm^2). However, the global layer

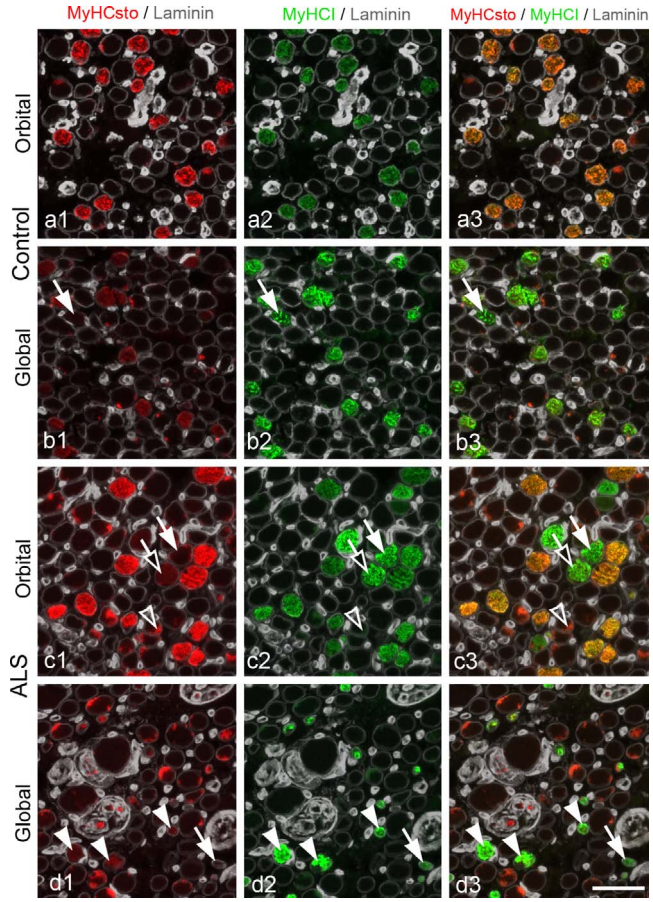

Figure 1. Immunofluorescence images of medial rectus cross sections in the orbital (**a1–a3**, **c1–c3**) and global (**b1–b3**, **d1–d3**) layer of a control (**a1–b3**) and an ALS subject (**c1–d3**) triple-labeled with antibodies against MyHCsto (*red*), MyHCI (*green*) and laminin (*gray*). Labeling with the antibodies against MyHCsto (*left*) was stronger in the orbital layer than in the global layer of both ALS and control subjects. In contrast, labeling with the antibody against MyHCI (*middle*) was consistently stronger in the global layer than in the orbital layer. Sporadic myofibers in both layers were labeled for MyHCI but were completely unlabeled with the antibody against MyHCsto (*white arrows*). In the orbital layer of ALS patients, a minority of myofibers had a labeling pattern where MyHCI reactivity was strong and MyHCsto reactivity was weak (*open arrows*). Notice the small CSA of myofibers labeled with the antibody against MyHCI in (**d1–d3**), and that labeling with the antibody against MyHCsto is seen in only two myofibers (*arrowheads*). The antibody against laminin labels the basal lamina of myofibers, capillaries, and nerve fascicles. Lipofuscin inclusions (exemplified with *open arrowheads*) are visible in red and green filters due to their autofluorescent properties, but are easily distinguished from true double-labeling by their distinct color in the merged pictures and by their morphology. *Scale bar*: 50 μm.

MyHCI+sto myofibers were significantly larger than the MyHCI myofibers in that layer ($P < 0.004$), whereas in the orbital layer there was only a trend ($P < 0.055$) for similar differences between CSAs.

MyHCI and MyHCsto in the ALS EOMs

As in control individuals, a difference in MyHCsto and MyHCI labeling was noted between the orbital and global layers. However, in ALS patients, a minority of myofibers (estimated to be less than 5%) in the orbital layer exhibited a different labeling pattern where MyHCsto labeling was weak and MyHCI labeling was strong (Fig. 1).

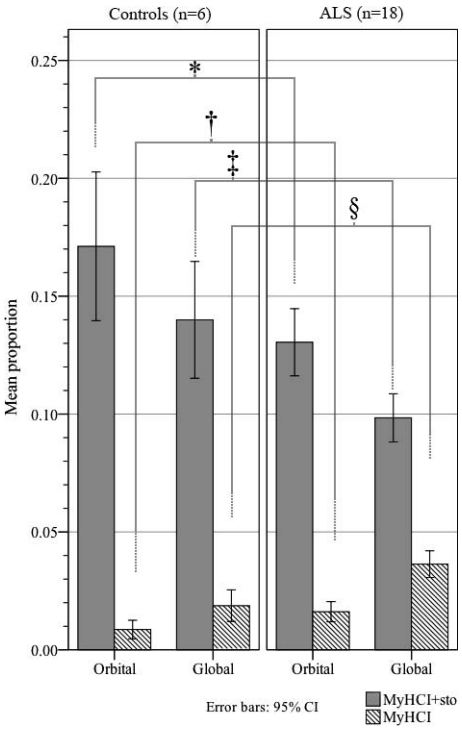

Figure 2. Bar graph showing the mean proportion of MyHCI+sto fibers (*gray bars*) and MyHCI-only (*striped bars*) myofibers related to the total number of myofibers in the orbital and global layer, respectively. *Significant difference ($P < 0.015$) in MyHCI+sto myofiber proportion between controls and ALS subjects in the orbital layer. †Significant difference ($P < 0.041$) in MyHCI-only myofiber proportion between control and ALS subjects in the orbital layer. ‡Significant difference ($P < 0.003$) in MyHCI+sto myofiber proportion between control and ALS subjects in the global layer. §Significant difference ($P < 0.009$) in MyHCI-only myofiber proportion between control and ALS subjects in the global layer.

In the medial rectus muscle of ALS patients, the proportion of double-labeled MyHCI+sto myofibers was significantly lower than in control subjects both in the global layer (9.8 ± 3.1 vs. 14.0 ± 2.4% in controls, $P < 0.002$) and in the orbital layer (13.0 ± 4.3 vs.17.1 ± 3.0% in controls, $P < 0.014$) (Fig. 2). There was no statistical difference between ALS patients with spinal-onset or bulbar-onset, but bulbar-onset patients had generally lower proportions of MyHCI+sto myofibers in both the global layer (8.6 ± 3.0 vs. 10.7 ± 3.0% in spinal-onset patients, $P < 0.13$) and orbital layer (11.1 ± 2.6 vs. 14.6 ± 4.8% in spinal-onset patients, $P < 0.08$). The proportion of MyHCI-only myofibers was significantly ($P < 0.007$) higher in ALS patients than in age-matched control individuals in the global layer (3.7 ± 1.7% in ALS vs. 1.9 ± 0.6% in controls), whereas in the orbital layer, there was only a trend ($P < 0.053$) in the same direction (1.6 ± 1.3% in ALS versus 0.8 ± 0.4% in controls).

As in healthy control subjects, a higher proportion of myofibers in the orbital layer than in the global layer was double-labeled for MyHCI+sto ($P < 0.002$). As in controls, the proportion of MyHCI-only myofibers in the global layer was higher than in the orbital layer ($P < 0.001$) in the ALS patients.

The mean CSA of MyHCI+sto myofibers in the orbital layer did not differ between controls and ALS individuals ($P < 0.371$; Fig. 3). In contrast to controls, where the mean CSA of MyHCI+sto fibers was very similar in the global and orbital layers, both spinal- and bulbar-onset ALS patients had significantly smaller MyHCI+sto myofibers in the global layer

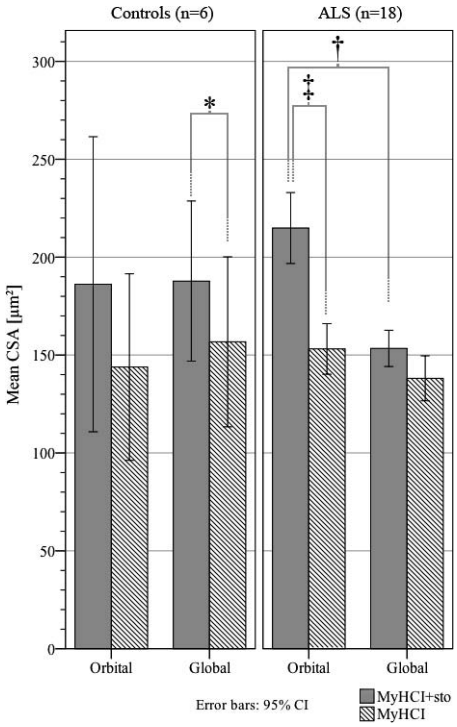

FIGURE 3. Bar graph showing the mean CSA of MyHCI+sto myofibers (*gray bars*) and MyHCI-only (*striped bars*) myofibers in the orbital and global layer, respectively, of control and ALS subjects. *Significant difference ($P < 0.004$) between MyHCI+sto and MyHCI-only myofibers in the global layer of controls. †Significant difference ($P < 0.001$) between the mean CSA of MyHCI+sto myofibers in the orbital and global layer, respectively, in the ALS patient group. ‡Significant difference ($P < 0.002$) between MyHCI+sto and MyHCI-only myofibers in the orbital layer of ALS patients. *P* values are adjusted for multiple comparisons with Sidak post hoc correction.

compared to the orbital layer (155 ± 33 vs. 234 ± 73 μm², $P < 0.024$ in bulbar-onset patients and 153 ± 23 vs. 200 ± 32 μm², $P < 0.010$ in spinal-onset patients). The difference in mean CSA between ALS and control subjects did not reach statistical significance ($P < 0.063$), but suggested that global layer MyHCI+sto myofibers may be smaller in ALS than in control individuals.

Two ALS patients with lower leg disease onset (patients 1 and 2) were siblings and homozygous carriers for the SOD1 D90A mutation. Despite their high genetic similarity (>50%), the clinical course varied notably between them, with patient 1 surviving twice as long as patient 2. Patient 1 (with a longer survival length) had a higher proportion of MyHCI+sto fibers (12.4%) with a similar mean CSA (151 μm²) as other ALS patients, whereas patient 2 (with a shorter survival length) had a considerably lower proportion of MyHCI+sto fibers (8.3%) that were also smaller in size (138 μm²).

Four ALS patients in the cohort had very long trinucleotide expansions in the gene *C9orf72*, a known genetic cause of ALS that can also give rise to frontotemporal dementia. Four C9orf72 patients constituted too few subjects for a statistical analysis, but some differences were noted. Two C9orf72 ALS patients with spinal onset (patients 3 and 4) had very short survival (<1 year) and normal proportions (13.2% and 13.3%, respectively) of MyHCI+sto in the global layer that were of similar mean CSA as in control subjects (201 and 179 μm², respectively). Another spinal-onset C9orf72 ALS patient (patient 7) with slower progression and signs of cognitive involvement had a somewhat lower proportion of MyHCI+sto

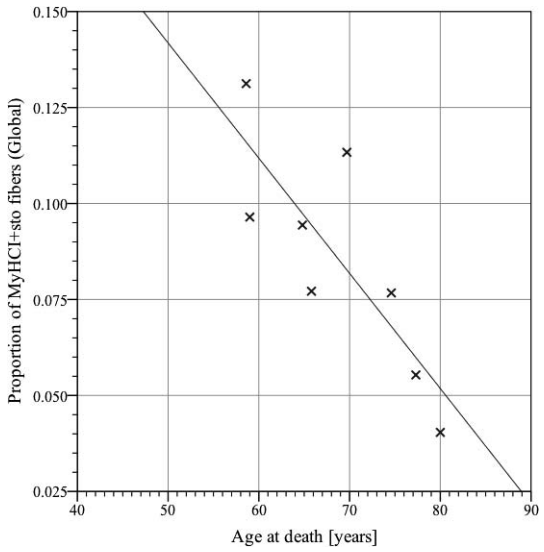

FIGURE 4. Proportion of MyHCI+sto myofibers in the global layer, as a function of age of death in bulbar-onset patients (*crosses*). *Line* represents best-fitting linear model. $R^2 = 0.669$ (unadjusted squared Pearson correlation coefficient). Model $\beta = -0.003$. The *F*-ratio of the overall model was significant, and the *P* value for the age of death coefficient in the bootstrap was $P < 0.019$, showing that the proportion of MyHCI+sto myofibers decreased with increasing age of death of the ALS bulbar-onset patients.

fibers in the global layer (10.0%) that were notably smaller (131 μm²). The fourth patient (number 16) had bulbar-onset ALS and even lower proportions of MyHCI+sto fibers in the global layer (7.7%) with the smallest mean CSA of all subjects studied in the cohort (118 μm²). The data on fiber proportion and mean CSA in the orbital layer of these four patients and the two D90A patients mentioned above were more varied and did not segregate clearly into different clinical phenotypes.

Correlations With Patient Age

ALS patients as a group had significantly lower proportions of MyHCI+sto fibers, especially in the global layer, this being the finding that most robustly separated ALS from control subjects. Simultaneously, there was a remarkable variation in proportions between individuals, varying between almost normal (13.1% in global layer of patient 11) and extremely low (4.0% in global layer of patient 18). Therefore, we investigated factors that could explain this variation in a regression analysis. We found that in bulbar-onset patients, but no other group, age of death (Fig. 4) correlated with a significant ($P < 0.019$) amount of variation in MyHCI+sto ($R^2 = 0.669$ for age of death) but practically none of the variation in the other two groups (Supplementary Fig. S1). Age of onset was borderline significant with a similar coefficient to the age of death regression. Interestingly, disease duration explained no variation in MyHCI+sto proportion for either group (Supplementary Fig. S2). The regression coefficient (β) for MyHCI+sto proportion as a function of age of death in years was −0.003 (bootstrap CI95%: −0.004 to −0.001). The population-adjusted R^2 was ≈0.479, implying that MyHCI+sto proportion and age of death should correlate well in bulbar-onset patient populations beyond our study cohort. In the case of estimating *P* values of age of onset as a dependent of MyHCI+sto proportion, convergence was difficult to achieve; even when performing in excess of 46,000 runs, the bootstrapped *P* value was inconsistent (range, 0.046–0.052) between individual runs.

Discussion

The major findings of the present study were (1) loss of MyHCI+sto fibers in both layers of the medial rectus in ALS patients; (2) increase in the proportion of myofibers labeled only for MyHCI and lacking MyHCsto in the global layer of ALS patients; (3) high correlation of age of death, but not disease duration, with loss of MyHCI+sto myofibers in the global layer of patients with bulbar onset of symptoms, but not in patients with spinal onset nor in controls.

A previous study[14] reported the normal fiber type distribution in the superior, lateral, and inferior rectus along with the superior oblique of healthy human subjects with a mean age of 37.5 years, whereas the current study focused solely on the medial rectus of older subjects (mean age 66.0 years). Despite these differences, the data from the two studies are similar, with the mean proportion of MyHCsto fibers in the previous study being 13% in the orbital layer and 16% in the global layer[14] and the proportions in the current study being 14% and 17%, respectively. Comprising a larger myofiber sampling and with an older group of subjects, the current study showed that myofibers labeled with only MyHCI were few, but approximately twice as prevalent in the global layer compared to the orbital layer, and that myofibers labeled with only MyHCI were approximately 20% smaller in size than myofibers labeled with both MyHC isoforms. The labeling patterns of MyHCI and MyHCsto were different in the orbital and global layers, with MyHCI labeling being particularly strong in the global layer and MyHCsto being particularly strong in the orbital layer. This could reflect a difference in epitope accessibility but could also reflect differences in the relative amount of MyHC isoforms present in these myofibers. The slow tonic MIFs of the global and orbital layers have previously been shown to have different electrophysiological properties[24] and different ultrastructural characteristics; for example, the orbital layer slow tonic myofibers have more mitochondria, more sarcoplasmic reticulum, and smaller myofibrils than slow tonic fibers in the global layer.[25] These functional differences could possibly also be reflected in different ratios of MyHC isoforms in the sarcomeres of these myofibers.

In addition to the significant loss of MyHCI+sto fibers in the global and orbital layers of ALS patients, there was a tendency for decrease in CSA in MyHCI+sto fibers in the global layer, suggesting that the global layer MyHCI+sto fibers of EOMs may be more severely affected in ALS. Although the patient group included a number of familial cases with known genetic causes of ALS (namely SOD1 missense mutations and C9orf72 nucleotide expansions), the numbers of patients were too low for a statistical comparison between groups with different forms of familial ALS. However, low proportions of global layer MyHCI+sto fibers were noted in individual patients from both familial forms of ALS, suggesting that loss of slow tonic fibers is a shared feature across different types of ALS.

Orbital MyHCI+sto fibers have been reported to react to acute mechanical denervation with a noticeable hypertrophy that can last for at least 3 months.[26] Similar results have also been demonstrated in chicken limb slow tonic myofibers.[27] However, hypertrophy of orbital MIFs has not been reported in response to bilateral botulinum toxin treatment, where only singly innervated fibers in the orbital layer undergo a transient hypertrophy.[28] This suggests that denervation-induced hypertrophy in the MyHCsto myofibers of EOMs may be dependent on the mechanism of denervation. Due to the transient and mechanism-dependent hypertrophy of orbital MyHsto myofibers in EOMs, it is difficult to study these changes in the context of ALS. The finding of an altered labeling of some MyHCI+sto fibers in the orbital layer raises the question whether these myofibers have maintained their innervation but shifted myofiber phenotype, or whether they reflect a new phenotype conveyed by reinnervation by another motor neuron. Motor neurons innervating slow type myofibers appear to have a high sprouting competence and seem to be the most resilient motor neurons of the spinal cord in ALS,[29,30] but the present results suggest that this may not be the case for motor neurons in the oculomotor nucleus that innervate slow myofibers in the EOMs.

The present study supports previous findings that EOMs are only partially spared in ALS[8] and raises questions regarding the impact of loss of MyHCI+sto myofibers on eye motility. Although we lack quantitative data on eye motility, the patients studied here had not reported difficulties with eye motility during the course of their disease. MyHCI+sto myofibers are thought to be responsible for fine-tuning of ocular movements, regulation during vergence, and possibly also smooth pursuit movements.[31] Two recent studies conclude that the majority of ALS patients have either no eye motility disturbance or show deficits only in the executive functions of eye movements.[32,33] One of the studies reported that maximum saccadic velocity is slightly decreased in a subgroup of ALS patients,[32] suggesting some involvement of the oculomotor nucleus. Those patients also display catch-up saccades during smooth pursuit movements, indicating damage to the neurons involved in these movements.[32] It remains to be determined whether saccade replacement of smooth pursuit movements may be linked to the loss of MyHCI+sto myofibers. The neuroanatomic segregation[16,17,34] of singly innervated fiber (SIF) motor neurons and MIF motor neurons in the oculomotor nucleus allows for future studies to link the changes in MIFs in the EOMs more directly to possible changes at the motor neuron level.

The strong association between age of death and loss of MyHCI+sto myofibers in bulbar-onset patients warrants some consideration of its validity before interpreting the results. First, all groups passed the statistical assumptions set up for the linear regression, and a visual inspection of Figure 4 reveals that the bulbar-onset patients line up in an orderly way around the regression slope. Secondly, while the correlational coefficient was very small in the control and spinal-onset groups ($R^2 = 0.037$ and $R^2 = 0.019$, respectively), it was unexpectedly large ($R^2 = 0.669$) in the bulbar-onset group, suggesting that this correlation is a distinct characteristic of this group. The notion that this age-dependent decline is inherently different from normal aging is supported by studies of the oculomotor system that show no decline in neurons with aging.[35,36] It is further supported by the minimal difference in proportion of myofibers labeled for MyHCsto between a previous study on younger human subjects[14] and those older control subjects reported here, suggesting that both MIFs of the EOMs and their motor neurons undergo very limited degenerative changes with normal aging. Thirdly, while ALS pathophysiology is complex and poorly understood, it has been noted previously that the correlation between aging and ALS is more pronounced in bulbar-onset cases.[37–39]

In summary, this study has established the degree of loss of MyHCsto myofibers in ALS with different types of onset, duration, and genetics. This could possibly explain the deterioration of smooth pursuit movements previously reported in some ALS patients. Also, this study strengthens the notion that bulbar-onset ALS is more intimately associated with aging processes than spinal-onset ALS. Importantly, it suggests that while eye motility is generally spared in ALS, subtle degenerative changes do occur at the terminal stage of the disease.

Acknowledgments

The authors thank Stefano Schiaffino for the generous gift of the antibody against MYH14/7b. The monoclonal antibody, A4.951, developed by Helen M. Blau, was obtained from the Developmental Studies Hybridoma Bank, created by the National Institute of Child Health and Human Development of the National Institutes of Health and maintained at the University of Iowa (Department of Biology, Iowa City, IA, USA).

Supported by grants from the Swedish Research Council (2015-02438), County Council of Västerbotten (Cutting Edge Medical Research; Central ALF), the Swedish Brain Research Foundation, The Knut and Alice Wallenberg Foundation, the Ulla-Carin Lindquist ALS Foundation, Neuroförbundet, and Stiftelsen Kronprinsessan Margaretas Arbetsnämnd för Synskadade (KMA).

Disclosure: **A.E. Tjust**, None; **A. Danielsson**, None; **P.M. Anderson**, None; **T. Brännström**, None; **F. Pedrosa Domellöf**, None

References

1. Zarei S, Carr K, Reiley L, et al. A comprehensive review of amyotrophic lateral sclerosis. *Surg Neurol Int*. 2015;6:171.
2. Charcot JM, Joffroy A. Deux cas d'atrophie musculaire progressive avec lesion de la subsance grise et des daisceaux anterolateraux de la moelle epiniere. *Arch Physiol Neurol Pathol*. 1869;744.
3. Cohen B, Caroscio J. Eye movements in amyotrophic lateral sclerosis. *J Neural Trans Suppl*. 1983;19:305–315.
4. Mizutani T, Aki M, Shiozawa R, et al. Development of ophthalmoplegia in amyotrophic lateral sclerosis during long-term use of respirators. *J Neurol Sci*. 1990;99:311–319.
5. Mizutani T, Sakamaki S, Tsuchiya N, et al. Amyotrophic lateral sclerosis with ophthalmoplegia and multisystem degeneration in patients on long-term use of respirators. *Acta Neuropathol*. 1992;84:372–377.
6. Lawyer T Jr, Netsky MG. Amyotrophic lateral sclerosis. *AMA Arch Neurol Psychiatry*. 1953;69:171–192.
7. Okamoto K, Hirai S, Amari M, et al. Oculomotor nuclear pathology in amyotrophic lateral sclerosis. *Acta Neuropathol*. 1993;85:458–462.
8. Ahmadi M, Liu JX, Brannstrom T, Andersen PM, Stal P, Pedrosa-Domellof F. Human extraocular muscles in ALS. *Invest Ophthalmol Vis Sci*. 2010;51:3494–3501.
9. Liu JX, Brannstrom T, Andersen PM, Pedrosa-Domellof F. Distinct changes in synaptic protein composition at neuromuscular junctions of extraocular muscles versus limb muscles of ALS donors. *PLoS One*. 2013;8:e57473.
10. Tjust AE, Brannstrom T, Pedrosa Domellof F. Unaffected motor endplate occupancy in eye muscles of ALS G93A mouse model. *Front Biosci (Schol Ed)*. 2012;4:1547–1555.
11. Fischer LR, Culver DG, Tennant P, et al. Amyotrophic lateral sclerosis is a distal axonopathy: evidence in mice and man. *Exp Neurol*. 2004;185:232–240.
12. Parkhouse WS, Cunningham L, McFee I, et al. Neuromuscular dysfunction in the mutant superoxide dismutase mouse model of amyotrophic lateral sclerosis. *Amyotroph Lateral Scler*. 2008;9:24–34.
13. Bormioli SP, Torresan P, Sartore S, Moschini GB, Schiaffino S. Immunohistochemical identification of slow-tonic fibers in human extrinsic eye muscles. *Invest Ophthalmol Vis Sci*. 1979;18:303–306.
14. Kjellgren D, Thornell LE, Andersen J, Pedrosa-Domellof F. Myosin heavy chain isoforms in human extraocular muscles. *Invest Ophthalmol Vis Sci*. 2003;44:1419–1425.
15. Teravainen H. Electron microscopic and histochemical observations on different types of nerve endings in the extraocular muscles of the rat. *Z Zellforsch Mikrosk Anat*. 1968;90:372–388.
16. Eberhorn AC, Ardeleanu P, Buttner-Ennever JA, Horn AK. Histochemical differences between motoneurons supplying multiply and singly innervated extraocular muscle fibers. *J Comp Neurol*. 2005;491:352–366.
17. Eberhorn AC, Buttner-Ennever JA, Horn AK. Identification of motoneurons supplying multiply- or singly-innervated extraocular muscle fibers in the rat. *Neuroscience*. 2006;137:891–903.
18. Tang X, Buttner-Ennever JA, Mustari MJ, Horn AK. Internal organization of medial rectus and inferior rectus muscle neurons in the C group of the oculomotor nucleus in monkey. *J Comp Neurol*. 2015;523:1809–1823.
19. Andersen PM, Abrahams S, Borasio GD, et al. EFNS guidelines on the clinical management of amyotrophic lateral sclerosis (MALS)–revised report of an EFNS task force. *Eur J Neurol*. 2012;19:360–375.
20. Rossi AC, Mammucari C, Argentini C, Reggiani C, Schiaffino S. Two novel/ancient myosins in mammalian skeletal muscles: MYH14/7b and MYH15 are expressed in extraocular muscles and muscle spindles. *J Physiol*. 2010;588:353–364.
21. Gundersen HJ, Bendtsen TF, Korbo L, et al. Some new, simple and efficient stereological methods and their use in pathological research and diagnosis. *APMIS*. 1988;96:379–394.
22. Bradley E. Better bootstrap confidence intervals. *J Am Stat Assoc*. 1987;82:171–185.
23. Claudy JG. Multiple regression and validity estimation in one sample. *Appl Psychol Meas*. 1978;2:595–607.
24. Jacoby J, Chiarandini DJ, Stefani E. Electrical properties and innervation of fibers in the orbital layer of rat extraocular muscles. *J Neurophysiol*. 1989;61:116–125.
25. Mayr R. Structure and distribution of fibre types in the external eye muscles of the rat. *Tissue Cell*. 1971;3:433–462.
26. Asmussen G, Kiessling A. Hypertrophy and atrophy of mammalian extraocular muscle fibres following denervation. *Experientia*. 1975;31:1186–1188.
27. Sola OM, Christensen DL, Martin AW. Hypertrophy and hyperplasia of adult chicken anterior latissimus dorsi muscles following stretch with and without denervation. *Exp Neurol*. 1973;41:76–100.
28. Spencer RF, McNeer KW. Botulinum toxin paralysis of adult monkey extraocular muscle. Structural alterations in orbital, singly innervated muscle fibers. *Arch Ophthalmol*. 1987;105:1703–1711.
29. Frey D, Schneider C, Xu L, Borg J, Spooren W, Caroni P. Early and selective loss of neuromuscular synapse subtypes with low sprouting competence in motoneuron diseases. *J Neurosci*. 2000;20:2534–2542.
30. Hegedus J, Putman CT, Tyreman N, Gordon T. Preferential motor unit loss in the SOD1 G93A transgenic mouse model of amyotrophic lateral sclerosis. *J Physiol*. 2008;586:3337–3351.
31. Ugolini G, Klam F, Doldan Dans M, et al. Horizontal eye movement networks in primates as revealed by retrograde transneuronal transfer of rabies virus: differences in monosynaptic input to "slow" and "fast" abducens motoneurons. *J Comp Neurol*. 2006;498:762–785.
32. Gorges M, Muller HP, Lule D, et al. Eye movement deficits are consistent with a staging model of pTDP-43 pathology in amyotrophic lateral sclerosis. *PLoS One*. 2015;10:e0142546.
33. Proudfoot M, Menke RA, Sharma R, et al. Eye-tracking in amyotrophic lateral sclerosis: a longitudinal study of saccadic and cognitive tasks. *Amyotroph Lateral Scler Frontotemporal Degener*. 2015;17:101–111.
34. Che Ngwa E, Zeeh C, Messoudi A, Buttner-Ennever JA, Horn AK. Delineation of motoneuron subgroups supplying individual eye muscles in the human oculomotor nucleus. *Front Neuroanat*. 2014;8:2.

Investigative Ophthalmology & Visual Science

35. Vijayashankar N, Brody H. A study of aging in the human abducens nucleus. *J Comp Neurol*. 1977;173:433–438.
36. Vijayashankar N, Brody H. Aging in the human brain stem. A study of the nucleus of the trochlear nerve. *Acta Anat (Basel)*. 1977;99:169–172.
37. Turner MR, Barnwell J, Al-Chalabi A, Eisen A. Young-onset amyotrophic lateral sclerosis: historical and other observations. *Brain*. 2012;135:2883–2891.
38. Chio A, Calvo A, Moglia C, Mazzini L, Mora G. Phenotypic heterogeneity of amyotrophic lateral sclerosis: a population based study. *J Neurol Neurosurg Psychiatry*. 2011;82:740–746.
39. Govoni V, Della Coletta E, Cesnik E, Casetta I, Granieri E. Can the age at onset give a clue to the pathogenesis of ALS? *Acta Neurol Belg*. 2017;117:221–227.

Investigative Ophthalmology & Visual Science